Journal of Achievements in Materials and Manufacturing Engineering
VOLUME 24
ISSUE 1
September
2007

Soft magnetic polymer-metal composites consisting of nanostructural Fe-basic powders

R. Nowosielski *
Institute of Engineering Materials and Biomaterials,
Silesian University of Technology, ul. Konarskiego 18a, 44-100 Gliwice, Poland
* Corresponding author: E-mail address: ryszard.nowosielski@polsl.pl

Received 19.03.2007; published in revised form 01.09.2007

Materials

ABSTRACT

Purpose: The paper presents and reviews the research results of soft magnetic composites consisting nanocrystalline powders obtained by soaking and high energetic milling of amorphous ribbons of metallic glasses $Fe_{78}Si_9B_{13}$ and $Fe_{73.5}Cu_1Nb_3Si_{13.5}B_9$.
Design/methodology/approach: Amorphous $Fe_{78}Si_9B_{13}$ and $Fe_{73.5}Cu_1Nb_3Si_{13.5}B_9$ ribbons were milled in a high energy ball mill (8000 SPEX CertiPrep Mixer/Mill) with a ball-to-sample weight ratio of 5:1. The obtained metallic powders were sieved to a particle mean diameter 200÷500 μm, 75÷200 μm and 25÷75 μm, and then annealed in an argon atmosphere to generate the nanocrystalline state. The powders particles were mixed and consolidated with polymer to obtain composites in the form toroidal cores. Observations of the structure of powders and composites were made on the Opton DSM-940 scanning electron microscope and electron transmitting microscope JEOL JEM 200CX and X-ray analysis. The X-ray tests were realized with the use of the XRD 7 SEIFERT-FPM diffractometer.
Findings: The analysis of the magnetic properties test results of the powders obtained in the high-energy ball of milling process, and the composites manufactured from these powders proved that the process causes significant decrease in the magnetic properties in relation to ribbons. The structure and magnetic properties of this material may be improved by means of a proper choice of parameters of this process as well as the final thermal treatment and first of all by decrease of demagnetization effect.
Research limitations/implications: For the powders, further magnetic, structure and composition examinations are planed.
Practical implications: The amorphous and nanocrystalline $Fe_{78}Si_9B_{13}$ and. $Fe_{73.5}Cu_1Nb_3Si_{13.5}B_9$ powders obtained by high-energy ball milling of metallic glasses feature an alternative to solid alloys and make it possible to obtain the ferromagnetic nanocomposites, whose shape, dimensions and magnetic properties can be freely formed in the determinate range.
Originality/value: The paper presents influence of chemical composition of selected Fe-based metallic glasses, annealing temperature and parameters of the high-energy ball milling process on structure and magnetic properties of soft magnetic powders materials obtained in this technique. This paper review also possibility of magnetic properties forming for metal-polymer nanocrystalline composites. Results and a discussion of the influence of high energy mechanical milling process on particle size and their distribution and annealing temperature of powders as well as structure and magnetic properties of investigated samples is presented. According to achieved results it has been attempted to describe the possibilities of improvement the soft magnetic properties of obtained Fe-based nanocrystalline powder materials and composites from them manufactured.
Keywords: Nanomaterials; Powders; Heat treatment; Magnetic properties; Magnetic composites

1. Introduction

In recent years, the Fe -based nanostructural (nanocrystalline) alloys has been intensively studied for its excellent soft magnetic properties [1÷10]. These nanostructural materials are prepared from amorphous ribbons approximately 20-50 μm thick produced by melt spinning method and next annealing or in form of powders by ball milling of metallic glasses ribbons or by mechanical alloying [1,11÷13]. The magnetic properties of the metallic glass ribbons and nanostructural materials depend on the chemical composition, production procedure and on the condition of the heat treatment (time and temperature) or parameters of ball milling [14÷16]. After annealing the ribbons of metallic glasses at above crystallization temperature for 1 hour in argon protecting atmosphere they become nanocrystalline. But due to process of rapidly solidification the shape of these alloys is limited practically to ribbons and wires (except bulk metallic glasses). The ribbon and wire geometries are very satisfactory for a range of applications, such as sensors and pulse generators, but are not the best for those in which large mass or volume of soft magnetic materials or complexly shaped soft magnetic part are required. Positive outcome of the amorphous – nanocrystalline transformation is the improvement of soft magnetic properties like very low coercitivity of less than 1 A/m, low AC losses and high magnetic saturation compared with amorphous materials. On the other hand, the ribbons of metallic glasses become very brittle, restricting its possible applications. Second disadvantage for many applications is the small thickness of ribbons and shapes of cores which are generally limited to toroidaly wound or stacked types [1÷10].

Obtaining powder nanocrystalline materials directly by grinding the metallic glasses makes it possible to carry out research on obtaining the ferromagnetic nanocomposites whose shape and dimensions may be formed freely [17÷25].

The composite with the polymer matrix reinforced with the amorphous or nanocrystalline particles obtained in the process of the high energy milling of the amorphous strips or mechanical alloying features the alternative for those materials.

Investigation of composite materials obtained by consolidation of the metallic powders using various methods is carried out in many research centers in the world [17÷25].

This solution encounters many difficulties, as particles with the length to diameter ratio of 1:1 (or close to it) run the significant risk of the demagnetising phenomenon.

In the case of soft magnetic a powder material, during the magnetisation of the short cylindrical sample, the saturation is achieved at the magnetic field intensity much grater than in the case when the close ring is used. It is caused by the fact that the intensity of the magnetic field (H_i) in the short sample is lower than the magnetic field (H) in the whole coil [23].

There is a relation between the magnetization (J) and the field intensity. When the partial demagnetization caused by the shape of the sample is taken into account, the relation may be presented in the following way:

$$J = \mu_0 \cdot H \cdot \frac{\kappa}{1 + \kappa N} \tag{1}$$

where:

N- demagnetization coefficient

k- magnetic susceptibility

μ_0 – induction constant (magnetic permeability of vacuum).

The N coefficient in the case of, for example, cylindrical samples depends mainly on the relation of sample length (l) to its diameter (D_p) [23].

$$p = \frac{l}{D_p} \tag{2}$$

The shorter and thicker the cylindrical rod is, the smaller value of the p parameter and at the same time the higher value of the (N) parameter is. The demagnetization effect of sample ends is presented in Fig.1.

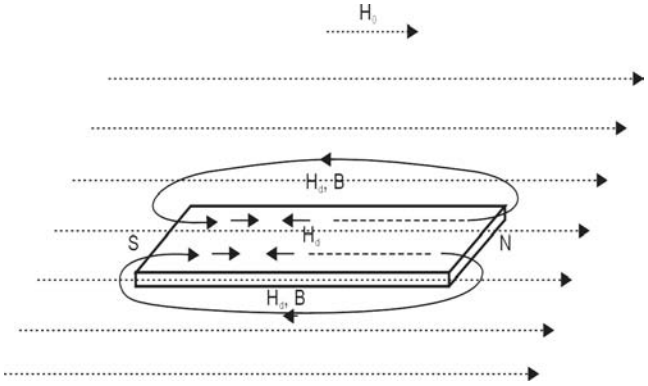

Fig. 1. The effect of demagnetisation of flat sample ends [23]

In addition, in case of the very small particles, below 1 μm the superparamagnetism phenomenon may occur. Both these phenomena deteriorate the soft magnetic properties of the obtained composites. Nevertheless, apart from the conventional heat treatment methods and heat treatment in the magnetic field, regulation is possible (in a certain range) of the magnetic and mechanical properties of the composite by selection and segregation of the powder grains according to their sizes and by selection of the mass portion of the polymer matrix.

The ball milling techniques of metallic glasses ribbons is often used to produce nanocrystalline soft magnetic material which is in powder form, and therefore is suitable for consolidation in a variety of shapes [14÷17]. Different consolidation techniques have been reported recently [16÷21]. The proposed procedures like sintering, hot isostating pressing, warm compaction, explosive compaction, shock – wave compaction and static high – pressure compaction with pressures up to 5 GPa are costly and complex. Processing of bulk materials from nanocrystalline powder (e.g. sintering) is very difficult due to the metastable state of nanocrystals. Annealing at high temperatures causes grain growth and soft magnetic properties decrease. That is why the most popular consolidation technique is mixing metallic powders with mineral or polymer binder [19÷25]. The optimization of the magnetic properties of nanocrystalline powder composites can be achieved by adjusting uniform packing density, the powder size, the volume binder rate, the nature of the binder and ideal orientation of powders particles in the cores.

The aim of this study is the preparation of toroidal shape nanostructural composite cores from high energy ball milled $Fe_{73.5}Cu_1Nb_3Si_{13.5}B_9$ powders and to investigate the powder particle size and content of polymer binder response of the soft

magnetic properties. The results of scanning electron microscopy (SEM), transmission electron microscopy (TEM) and X-ray diffraction (XRD) of the obtained powders is also presented.

The amorphous and nanocrystalline materials arouse interest of scientists in research centers all over the world in the last tree decades. This is connected with the soft magnetic properties characteristic for these materials and with the possibility of using them in the electronic and electrical industry [1÷4].

The metallic amorphous and nanocrystalline materials obtained by crystallization of the metallic glasses are available in the form of thin ribbons only, and their magnetic properties can be controlled by heat- or thermo-magnetic treatment. These limitations are complicated in addition by the feasibility of manufacturing only toroidal cores from the ribbons.

Obtaining the nanocrystalline metal powders by milling of metallic glasses features an alternative to solid materials like amorphous and nanocrystalline ribbons and makes it possible to obtain the ferromagnetic nanocomposites, whose shape and dimensions can be freely formed using various consolidation methods [14÷25].

2. Materials and methods

Amorphous $Fe_{78}Si_9B_{13}$, $Fe_{73.5}Cu_1Nb_3Si_{13.5}B_9$, metallic glasses ribbons (fig.2,3), were prepared by the melt spinning method. The width and thickness of these ribbons were 9-10.2 mm and 28-29 μm, respectively. A Thermolyne F6020C resistance muffle furnace was used for isothermal soaking of the amorphous ribbons and the powder. Soaking was carried out at temperature range 373-873 K for 1 hour in an argon protective atmosphere.

The annealed ribbons of metallic glasses were cut into small pieces of about 5 mm transverse dimension. These particles were sealed in a cylindrical stainless steel container under an Ar atmosphere. The ball milling process was performed in a high energy ball mill (8000 SPEX CertiPrep Mixer/Mill) with a ball-to-sample weight ratio of 5:1. The milling process reduced the starting material pieces (metallic glasses) to powder form. The metallic powder particles were sieved to obtain different sizes – small with average particles diameter between 25 to 75 μm, medium particles 300÷500 μm and the large ones between 750÷1200 μm. Obtained powders were mixed then with different contents of binder and condensed on mechanical shaker. As a binder, a silicone polymer Dublisil 20 from Dreve-Dentamid GMBH and other polymer materials was used.

The powder particles to silicon polymer weight ratios were 6:1, 5:1, 4:1, 3:1, 2:1 and 1:1 respectively. The toroidal cores so obtained had its external diameter of 34 mm, internal diameter of 28 mm and height of 8 mm. Fig. 1 shows the consolidated samples of toroidal cores.

X-ray examination of metallic ribbons and obtained powders was made using a XRD-7 (SEIFERT-FPM) diffractometer with a Co anode, producing radiation of λ = 0.17902 nm wave length. The X-ray tube was supplied with the current I = 40 mA under the voltage of U = 35 kV. Diffraction examinations were performed within the range of angles 2θ from 20 to 120 degrees. The measurement step was of 0.2° in length whilst the pulse counting time was 10 s.

The size of crystallites was determined using the Scherrer formula [1].

The morphology of the powder samples was observed by scanning electron microscopy OPTON DSM 940.

Examination of powders and composite cores magnetic properties (hysteresis loops) were carried out on the Lake Shore Cryotronics VSM vibration sample magnetometer with a maximum applied magnetic field of 800 kA/m. The permeability of the powders and composites cores was made on the Ferrometr device.

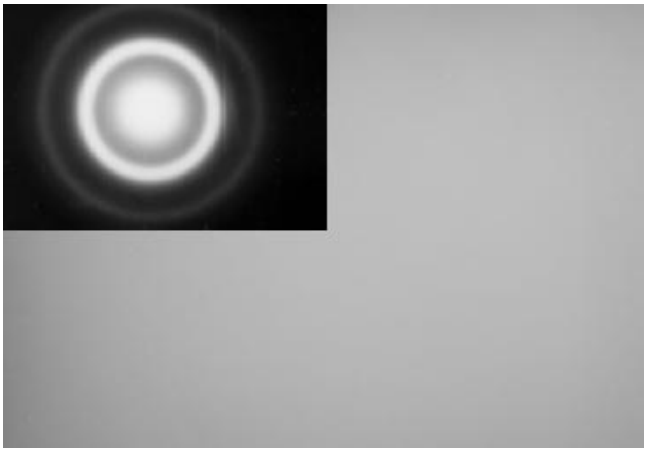

Fig.2. Amorphous structure of a $Fe_{78}Si_{13}B_9$ alloy; TEM micrograph at 60,000 x.

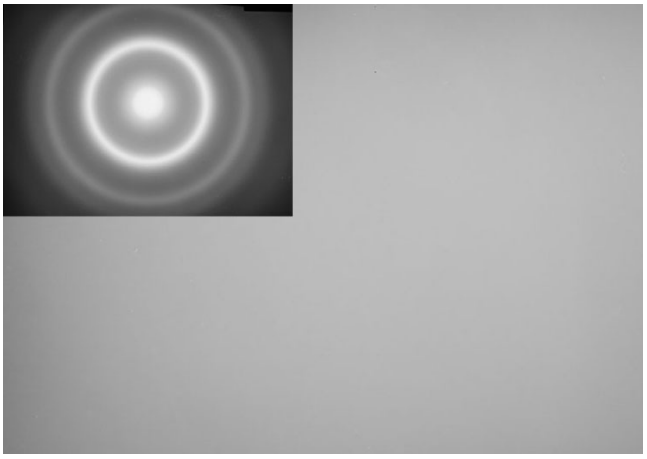

Fig.3. Transmission electron microscopy bright field image and selected area electron diffraction pattern of as-quenched $Fe_{73.5}Cu_1Nb_3Si_{13.5}B_9$ ribbon

Transmission electron microscopy (TEM) micrographs and selected area electron diffraction (SAED) patterns of the metallic ribbons and powders particles were obtained with a Joel Electron Microscope 200 CX. A disk-shaped sample of the ribbons and powders composites, 3 mm in diameter, were thinned with a GATAN-691 precision ion polishing system and than placed in the lateral entrance goniometry of the microscope, operating at 200kV.

3. Structure and properties of powders

Both milling method of metallic glasses ribbons: directly as quenched state and after annealing, conducted to getting powders with nanocrystalline structure (nanostructural powders) with different combination of phase composition; amorphous, Fe-α or α - Fe(Si) and borides, with different size of powders particles and different size of nanocrystalls in amorphous matrix, depend from time of milling and time and temperature of soaking of metallic glasses ribbons.

The morphology of the sieved powders obtained by milling amorphous ribbons examined by scanning electron microscopy (SEM) showed significant differences in the shape and size of powder particles in relation to the milling time. It is important because influence for the demagnetization effect and magnetic properties of powders. Fig. 4 A,B,C shows SEM images of $Fe_{78}Si_9B_{13}$ powder particles sieved to obtain different sizes – small with average particles diameter between 25 to 75 μm, medium particles 75÷200 μm and the large ones between 200÷500 μm Fig.4 D,E,F shows SEM images of $Fe_{73,5}Cu_1Nb_3Si_{13,5}B_9$ powder particles sieved to obtain different sizes – small with average particles diameter between 25 to 75 μm, medium particles 300÷500 μm and the large ones between 750÷1200 μm.

It was found that larger powder particles had shape like flakes as well as plates with sharp edges. Their thickness was much smaller than dimensions in two remaining directions. Shape of medium particles was also similar to the shape of flakes. Powders with average particles diameter between 25 to 75 μm had very different shape – irregular flakes, flat with round edges and perfect spherical shape, suitable for forming consolidated powder cores with high density. It was also found that some of the powder particles were agglomerated.

The average particle size for the $Fe_{78}Si_9B_{13}$ powder in the particle size distribution curve was for small particles (25÷75 μm) about d = 48 μm, for medium particles (75÷200 μm) about d = 127 μm and for the large ones (200÷500 μm) about d = 326 μm. For example the average particle size for the $Fe_{73,5}Cu_1Nb_3Si_{13,5}B_9$ powder in the particle size distribution curve was for small particles (25÷75 μm) about d = 58 μm, for medium particles (300÷500 μm) about d = 385 μm and for the large ones (750÷1200 μm) about d = 980 μm (Fig.5)

To obtain information about the crystalline phases an X-ray diffraction study (Fig.6) was carried out for the base sample ($Fe_{78}Si_9B_{13}$ metallic glass) for ball milled ribbon and for obtained powders annealed in Ar for 1h at temperature of 773 K.

It was found for the rapidly quenched ribbon the occurrence of a wide diffraction spectrum within the range of $2\theta = 45 \div 58^{o}$, being that phenomenon characteristic for an amorphous structure of iron alloys (A in Fig. 6). Fig 6 (B) shows the X-ray diffraction pattern for amorphous $Fe_{78}Si_9B_{13}$ powders. Fig 6 (C) shows the X-ray diffraction pattern for nanocrystalline $Fe_{78}Si_9B_{13}$ powders annealed in Ar for 1h at temperature of 773 K. There was a sharp peak with high intensity observed in the curve for the angle $2\theta = 52.8°$ being the characteristic angle for the α-Fe(Si) (110) plane reflection. Also (200) and (211) diffraction peaks of α-Fe(Si) were noticed.

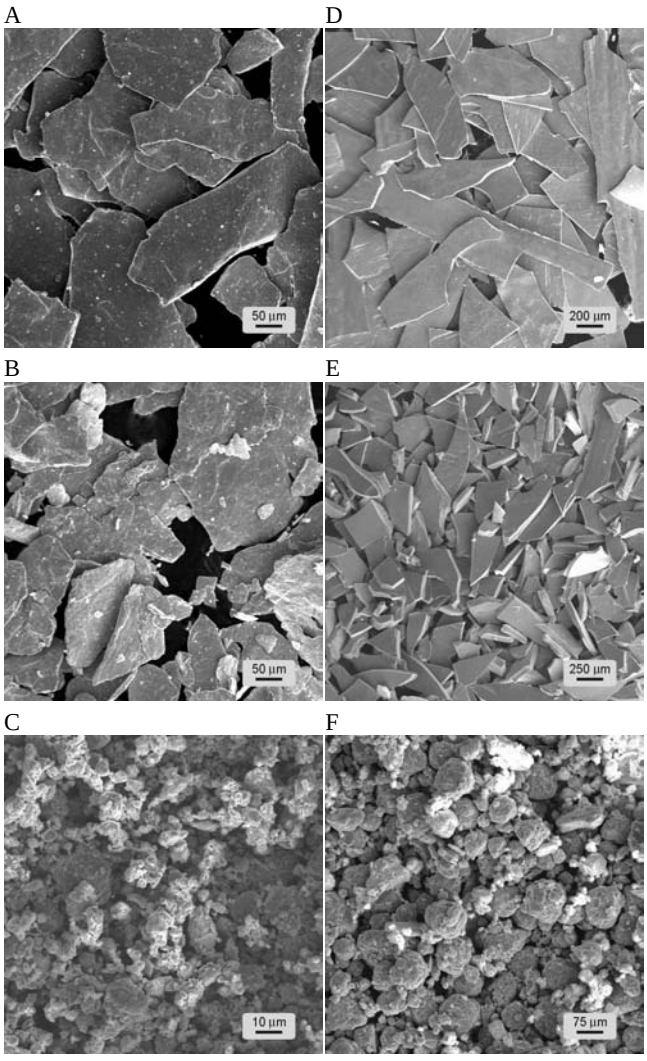

Fig. 4. SEM images of the $Fe_{78}Si_9B_{13}$ and $Fe_{73,5}Cu_1Nb_3Si_{13.5}B_9$ Respectively powders sieved on fractions between: (A) 200÷500 μm, (B) 75÷200 μm, (C) 25÷75 μm (D) 750÷1200 μm, (E) 300÷500 μm, (F) 25÷75 μm

Similar X-ray investigations performed for $Fe_{78}Si_9B_{13}$ and $Fe_{73.5}Cu_1Nb_3Si_{13.5}B_9$ powders manufactured by high energetic milling of metallic glasses ribbons showed similar results as above mentioned what very good illustrate Fig.7,8.

After 50 hours of $Fe_{78}Si_9B_{13}$ metallic glasses ribbon the existence of amorphous and α-Fe(Si) phases, which share changing with the time of milling. After 100 hours of milling probably advance process of amorphous phase crystallization occurring. Opposite is for $Fe_{73.5}Cu_1Nb_3Si_{13.5}B_9$ metallic glasses ribbon where after 100 hours milling very small changes are observed, which is evidence that structure is further amorphous.

The average crystallite size in the obtained powder was determined from the half maximum intensity breadth of the dominant peak of the X-ray diffraction pattern, using the Scherrer formula and amounts about 20-33 nm.

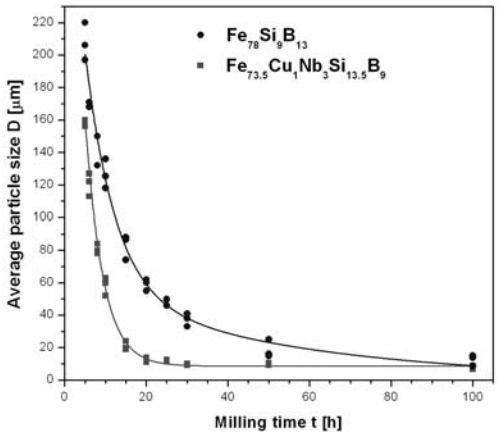

Fig.5. Average diameter of powder particles vs. milling time of metallic glasses ribbons

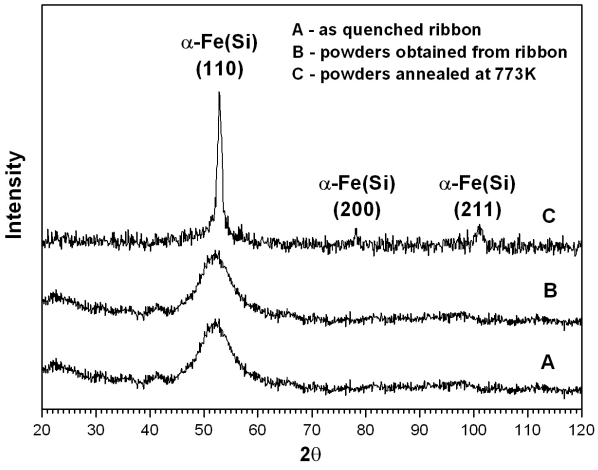

Fig 6. X-ray diffraction patterns of $Fe_{78}Si_9B_{13}$ samples: as quenched ribbon; (B) powders obtained from ribbon; (C) powders annealed at 773 K for 1 hour

After soaking the $Fe_{73,5}Cu_1Nb_3Si_{13,5}B_9$ material at 823 K for 1 hour, a high-energy grinding was carried out for 1, 2, 3, 4 and 5 hours respectively. A nanocrystalline powder was obtained as a result of the combination of thermal nanocrystalline and milling processes. The size of crystallites so obtained in the powder were function of time milling, and were smaller for longer time of milling (Fig.9), and share of crystalline and amorphous phases was also changing.

It was also found, that in high-energy milling of the amorphous $Fe_{78}Si_{13}B_9$ alloy strip soaked at 450°C for 1 hour, the intensity of the Fe-α diffraction lines decreases whilst small peaks from the Fe_3B and Fe_2B phases appeared (Fig. 10).

Generally from this experiment we can conclude that is possible to fabricate nanocrystalline powders from metallic glasses with different size of powder particles and different structure of powders by the use of a combined thermal nanocrystallization and high-energy milling, and this way we can minimize production time of determine powders.

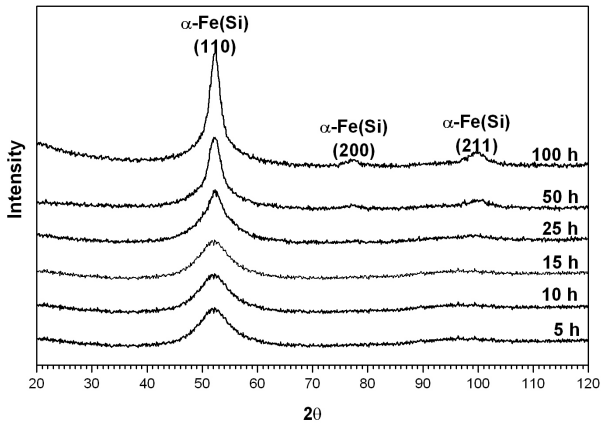

Fig.7. A set of x-ray diffractions for powders fabricated from the $Fe_{78}Si_{13}B_9$ metallic glasses strip for different time of milling

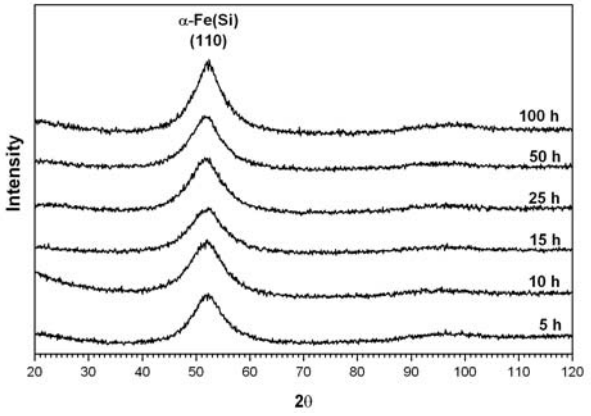

Fig.8. A set of x-ray diffractions for powders fabricated form the $Fe_{73.5}Cu_1Nb_3Si_{13.5}B_9$ metallic glasses strip for different time of milling

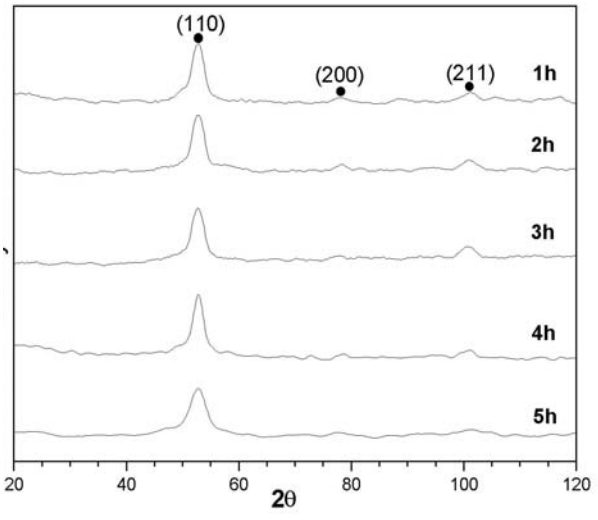

Fig. 9. X-ray diffraction patterns of $Fe_{73.5}Cu_1Nb_3Si_{13.5}B_9$ alloy the annealed sample at 823 K and milled for 1, 2, 3, 4, 5 hours

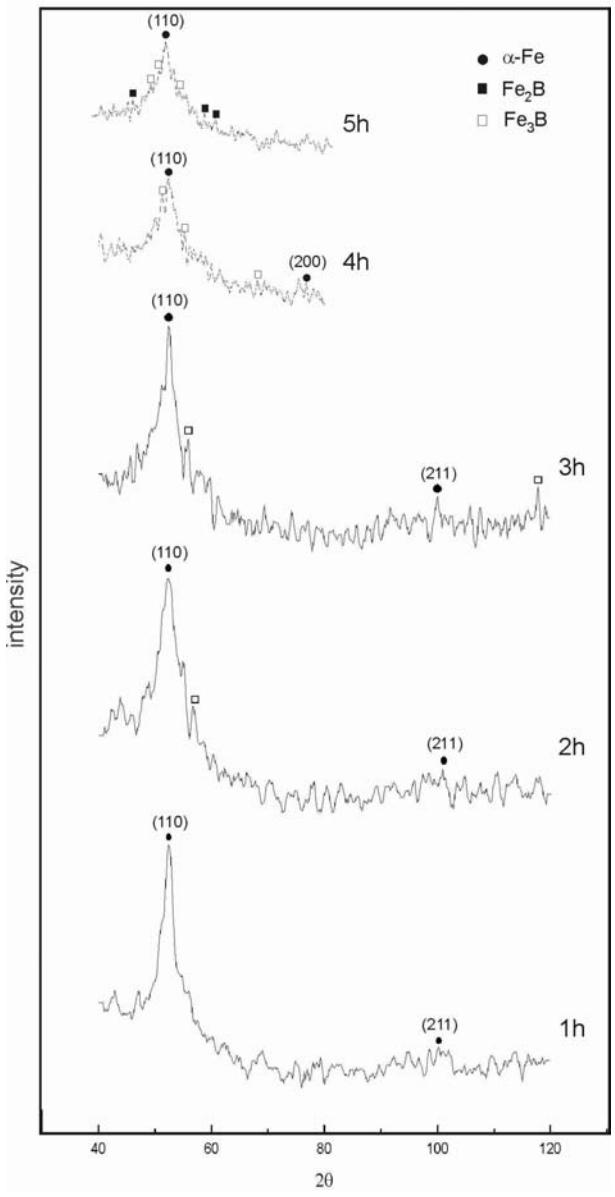

Fig.10. A set of diffractograms for powders fabricated frorm an amorphous $Fe_{78}Si_{13}B_9$ alloy strip soaked at 450°C for 1 hour

Fig.11 shows the transmission electron microscopy (TEM) microstructure image and the corresponding selected area electron diffraction (SAED) pattern of the ball milled $Fe_{78}Si_9B_{13}$ sample annealed in Ar for 1h at temperature of 773 K. The TEM image demonstrated nanocrystallits with a size around 20 nm embedded in an amorphous matrix.
It was consistent with SAED pattern, which exhibited diffraction rings for the (110), (200) and (211) of α-Fe(Si) phase and a diffuse amorphous ring (Fig.12). The phases identified by TEM were a good agreement with XRD analysis results.

Transmission electron microscopy (TEM) observation of the as-quenched $Fe_{73.5}Cu_1Nb_3Si_{13.5}B_9$ ribbon confirmed that the microstructure of the sample is very uniform. The bright field image shows a homogeneous material with no crystalline grains. Also, there is no trace of crystalline reflections in the selected area electron diffraction (SAED) pattern. These factors indicated that the as-quenched ribbon is fully amorphous.

Fig.13 shows the TEM microstructure image and the corresponding selected area electron diffraction (SAED) pattern of the ball milled $Fe_{73,5}Cu_1Nb_3Si_{13,5}B_9$ sample (previously annealed in Ar for 1h at temperature of 823 K). The phases identified by TEM were a good agreement with XRD analysis results.

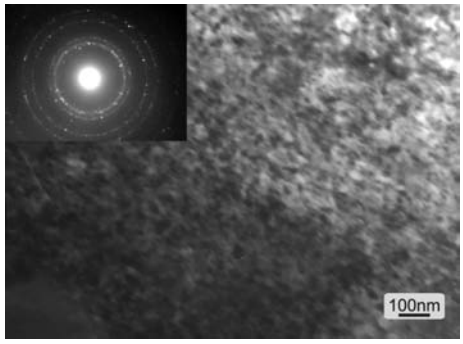

Fig. 11. Structure of a $Fe_{78}Si_{13}B_9$ alloy soaked at 450 °C/1 hour; TEM micrograph.

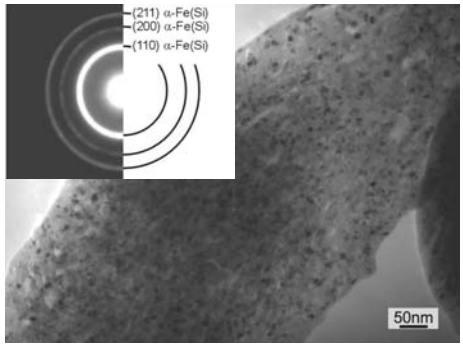

Fig 12. Transmission electron microscopy bright field image and selected area electron diffraction pattern of $Fe_{78}Si_9B_{13}$ powders annealed at 773 K for 1 hour.

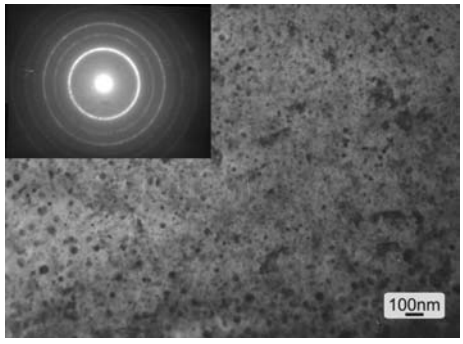

Fig 13. Transmission electron microscopy bright field image and selected area electron diffraction pattern of powders obtained from $Fe_{73.5}Cu_1Nb_3Si_{13.5}B_9$ ribbon annealed at 823 K

The saturation induction B_s, remanence B_r and coercive field H_c were determined from magnetic hysteresis loops of powders measured in a VSM for powders $Fe_{78}Si_9B_{13}$ and $Fe_{73.5}Cu_1Nb_3Si_{13.5}B_9$ with different structure produced by different methods and at different parameters (for example Fig.14,15).

Very interesting from the point of view demagnetization effect is examination of the magnetic properties of the both alloys powders as a function of particles size. For the $Fe_{78}Si_9B_{13}$ powders were found that the larger powder particles (200 ÷ 500 μm) exhibits better soft magnetic properties than the small ones i.e. the coercive field H_c = 1341 [A/m], B_s = 1.06 [T] and B_r = 0.068 [T]. Decreasing the particles size to 75 ÷ 200 μm decreased the B_s = 0.98 [T] and B_r = 0.061 [T]. Also increasing of coercive field up to 1920 [A/m] was observed. For small particle size (25 ÷ 75 μm) powder sample demonstrated the value of B_s = 0.72 [T] and the remanence B_r = 0.048 [T], whilst H_c = 3215 [A/m].

The permeability value of large and medium powder particles (measured at magnetic field H = 3 [kA/m] and at frequency f = 50 Hz) are μ = 39 and μ = 18 respectively. Annealing powders particles at 773 K produces the effect of a considerable increase of their magnetic properties. For large particles the value of coercive field was equal to 237 [A/m], B_s = 1.22 [T], B_r = 0.09 [T] and the permeability exhibited value of 106 (Fig.16).

Similar investigation of the magnetic properties of the $Fe_{73.5}Cu_1Nb_3Si_{13.5}B_9$ alloy powders with different particles size also showed that the larger powder particles exhibits better soft magnetic properties than the small ones i.e. the coercive field H_c = 13.75 [A/m], the saturation induction B_s = 1.21 [T] and the remanence B_r = 0.007 [T]. Decreasing the particles size to 300 ÷ 500 μm decreased the saturation induction down to B_s = 1.06 [T] and B_r = 0.006 [T]. Also increasing of coercive field up to 115.3 [A/m] was observed (Fig.17). For small particle size powder sample demonstrated the value of B_s = 0.64 [T] and the remanence B_r = 0.0038 [T], whilst H_c = 163.2 [A/m].

The permeability value of large and medium powder particles (measured at magnetic field H = 3 [kA/m] and at frequency f = 50 Hz) are μ = 175 and μ = 143 respectively.

For both alloys powders the magnetic permeability measurements confirmed better magnetic properties of powder particles, which had shape like flakes.

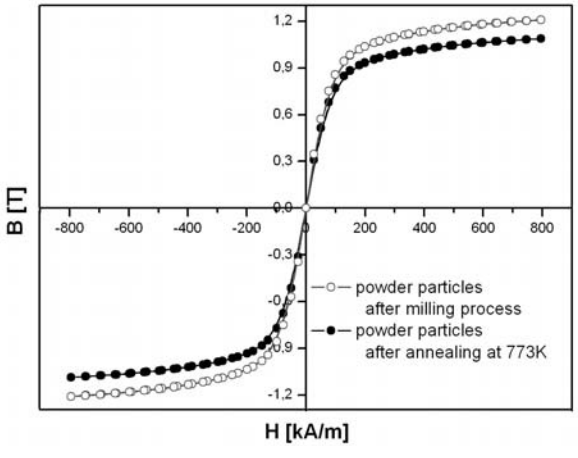

Fig. 14. Hysteresis loops for $Fe_{78}Si_9B_{13}$ powder particles (200 ÷ 500 μm) size, in as milled state and after annealed at 773K for 1 hour

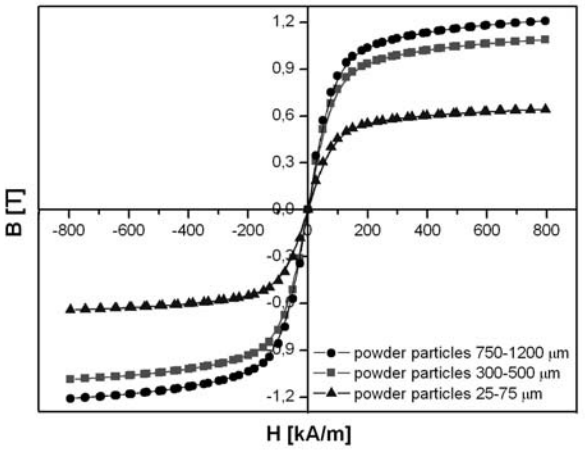

Fig. 15. Hysteresis loops for $Fe_{73,5}Cu_1Nb_3Si_{13,5}B_9$ alloy powders with different particles size

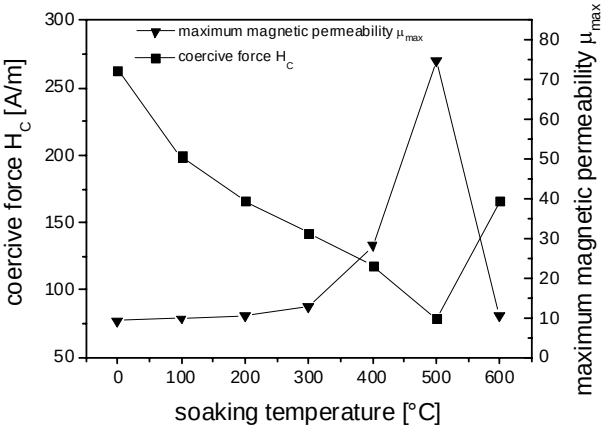

Fig. 16. The influence of the soaking temperature on the coercive force H_c and the maximum magnetic permeability μ_{max} of a $Fe_{78}Si_{13}B_9$ alloy powders.

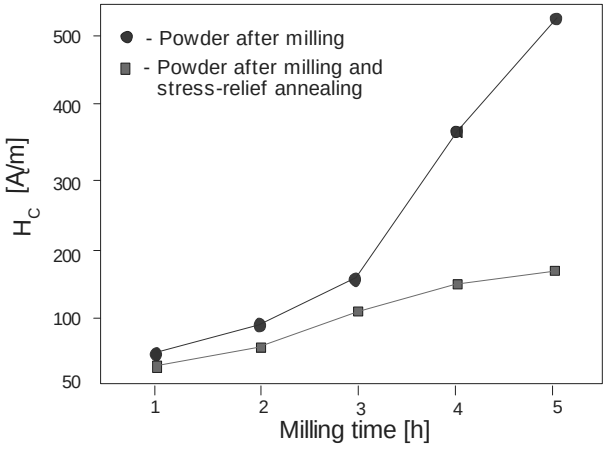

Fig. 17. The influence of the milling time on the coercive force H_c of the $Fe_{73.5}Cu_1Nb_3Si_{13.5}B_9$ alloy powders.

4. Composites research results and discussion

The investigations of magnetic properties performed for metal-polymer composites, consisting above described powders showed very strong relation of powder particle size and share of ferromagnetic phase on magnetic properties of composites. The structure and level of powders magnetic properties influence weaker for magnetic properties of composites.

The results of examination of the magnetic properties of the nanocomposite cores with different powder-to-silicone polymer ratio are shown in Fig. 18-23.

The coercive field (Fig.18,19) and the saturation induction (Fig. 20,21) of powder composite cores in dependence on the powder particles content (wt %) are compared.

The nanocrystalline cores with powder particles between 750÷1200 μm exhibited high value of saturation induction and coercive field was comparable for the powders obtained from ball milled ribbon previously annealed in argon protecting atmosphere for 1h at temperature of 823 K. The results of experimental studies demonstrated a correlation between the growing powder-to-silicon polymer ratio and the improvement of the magnetic properties of the composite.

The composite core with a powder particle content of 85.7 wt% exhibit H_c=83.2 [A/m], B_s=1.09 [T] and B_r=0.0058 [T]. Further decrease powder-to-silicon polymer ratio leads to deterioration of the magnetic properties, i.e. the coercive field goes considerably high at small values of both the remanence and the saturation magnetic induction: for example, for a composite core with a polymer content of 50 wt%, B_r=0.0049 [T], B_s=0.95 [T] whilst the coercive field 214.3 [A/m].

By decreasing the particles size fraction to 300÷500 μm the coercive field of composite core with powder particle content of 75 wt% is increased at low values of both the remanence and the saturation magnetic induction. For medium particle size, composite cores with different content of polymer binder showed H_c in the range 163÷267 [A/m], the values of B_s between 0.88÷0.97 [T] and the remanence B_r in the range 0.0048÷0.0054 [T].

Toroidal cores filled with small powder particles (25÷75 μm) demonstrated worse magnetic properties than the other samples. At 85.7 wt% powder the coercive field H_c was equal 238.1 [A/m], B_s=0.62 [T] and B_r=0.0032 [T].

Decreasing powder content to 50 wt% decreased the value of B_s to 0.51 [T] and B_r to 0.0024 [T], whilst H_c=311.4 [A/m].

The magnetic permeability measurements confirmed better magnetic properties of nanocomposite cores with powder particles between 750÷1200 μm (Fig. 23). These data represent the highest reported permeability (measured at magnetic field H=3 [kA/m] and at frequency f=50 Hz) μ=123 for core with $Fe_{73.5}Cu_1Nb_3Si_{13.5}B_9$ powder particle content of 85.7 wt%.

The medium powder particles (300÷500 μm) in the composite cores showed permeability between 64 and 106 depending on the powder-to-silicon polymer ratio. It was also found that for powder particles size between 25÷75 μm, composite cores with different content of polymer binder showed permeability in the range 20÷48 (measured at magnetic field H=3 [kA/m] and at frequency f=50 Hz).

Magnetic properties very strong depend from the demagnetization effect (powder grain size and shape) then from structure of powders particles, therefore impossible is to rich for polymer-metal composites similar magnetic properties as for winded cores of metallic glasses or nanostructural ribbons. However we can have other advantages from polymer-metal magnetic composites; possibilities of easy forming different shapes of magnetic cores, and much lower the active power losses (Fig.24,25).

5. Conclusions

The experimental studies showed that a combined process involving the thermal nanocrystallization and high-energy ball milling applied to an $Fe_{78}Si_9B_{13}$ and $Fe_{73.5}Cu_1Nb_3Si_{13.5}B_9$ alloys provided a solution to obtain a metallic powder containing α-Fe(Si) crystallites with a size around 20 nm embedded in an amorphous matrix. This two phase structure, present in the powder obtained by ball milling of nanocrystalline ribbons, was the optimal structure from magnetic properties point of view.

It was found that size and shape of the powder particles were responsible for soft magnetic properties of powder cores. Decreasing size of powder particles led to magnetic hardening of nanocrystalline $Fe_{78}Si_9B_{13}$ and $Fe_{73.5}Cu_1Nb_3Si_{13.5}B_9$ alloys. The main reason for the worse magnetic properties of small particles was high demagnetization factor. Additionally, structural defects induced during ball milling process of small particles also caused deterioration of magnetic properties.

The control of the soft magnetic properties of composite cores consolidated from nanocrystalline powders and silicone polymer binder can be achieved by adjusting powder particle size and powder-to-silicon polymer ratio.

It was found that composite cores fabricated from silicon polymer-solidified $Fe_{78}Si_9B_{13}$ and $Fe_{73.5}Cu_1Nb_3Si_{13.5}B_9$ nanocrystalline powders exhibits magnetic properties that strengthen with the growing metallic powder-to-silicon weight or volume ratio.

The best results (H_c=83.2 [A/m], B_s=1.09 [T], B_r=0.0058 [T] and μ=123 measured at magnetic field H=3 [kA/m] and at frequency f=50 Hz) were obtained for the composite core filled with powder particles between 750÷1200 μm and with a powder particle content of 85.7 wt%. These results are similar as for composites investigated by other authors for polymer-metal composites manufactured without pressing (Fig.26).

Magnetic properties (particularly magnetic permeability) very weak depend from initial magnetic permeability of metallic glasses ribbons used to this investigation.

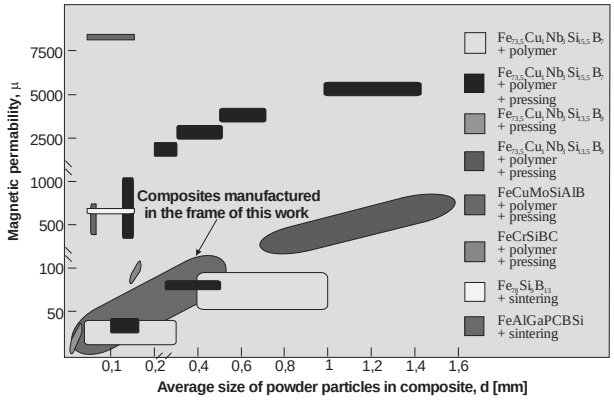

Fig.26. Magnetic permeability as a function of average powder particles size for polymer-metal composites manufactured by different technologies.

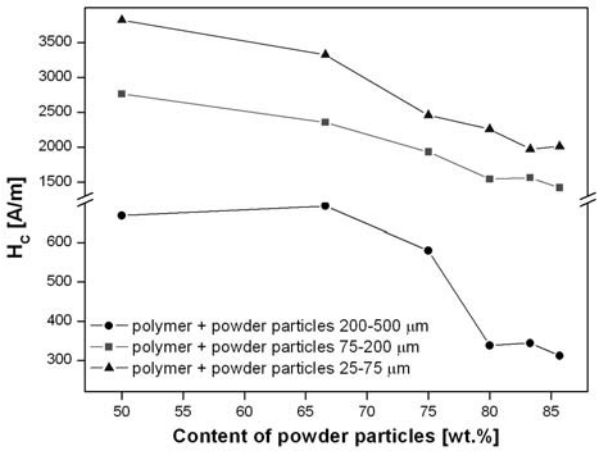

Fig. 18. Influence of the content of Fe78Si9B13 powder particles on the coercive field of composite cores

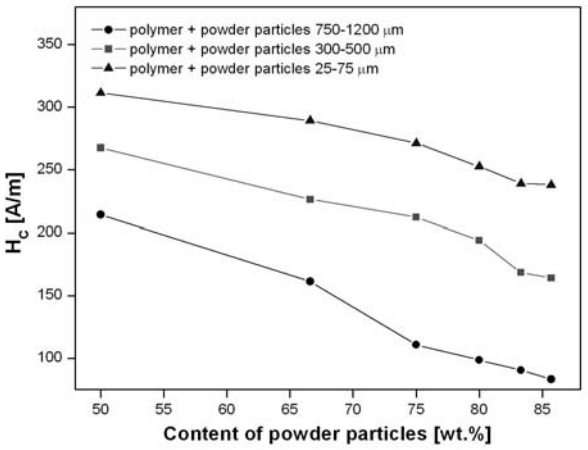

Fig. 19. Influence of the content of Fe73.5Cu1Nb3Si13.5B9 powder particles on the coercive field of composite cores

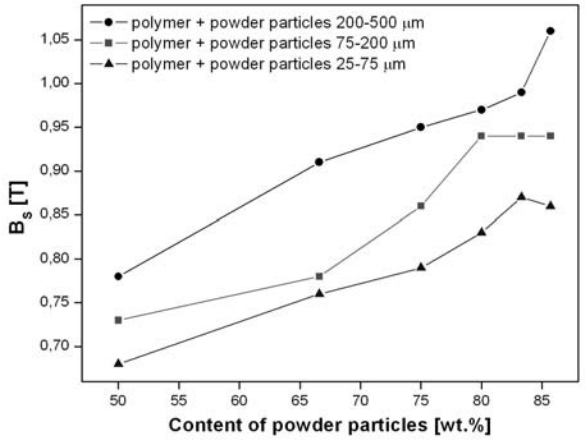

Fig. 20. Influence of the content of Fe78Si9B13 powder particles on the saturation induction of composite cores

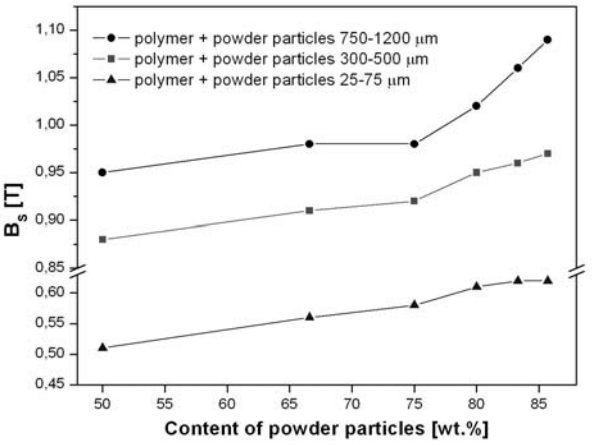

Fig.21. Influence of the content of Fe73.5Cu1Nb3Si13.5B9 powder particles on the saturation induction of composite cores

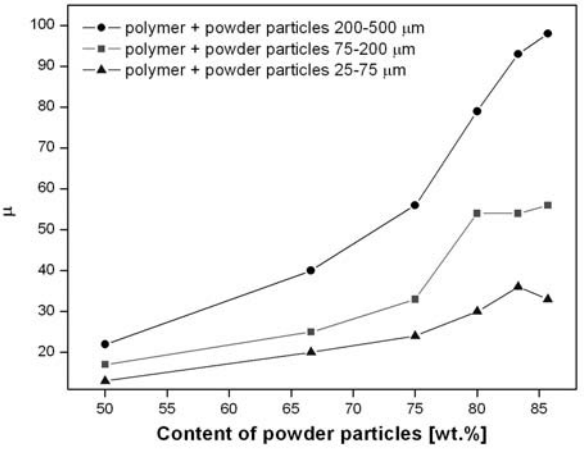

Fig.22. Influence of the content of Fe78Si9B13 powder particles on the magnetic permeability of composite cores

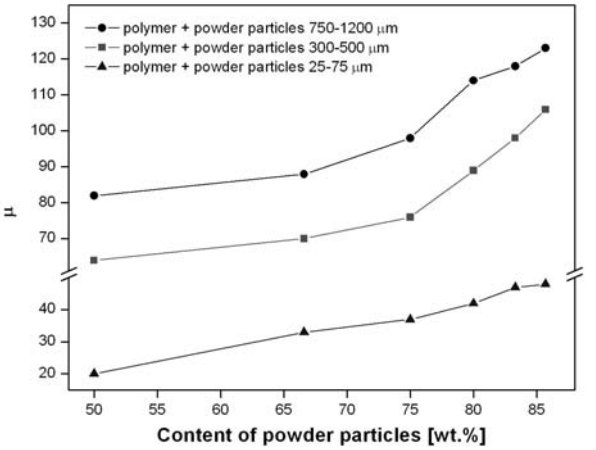

Fig. 23. Influence of the content of Fe73.5Cu1Nb3Si13.5B9 powder particles on the magnetic permeability of composite cores

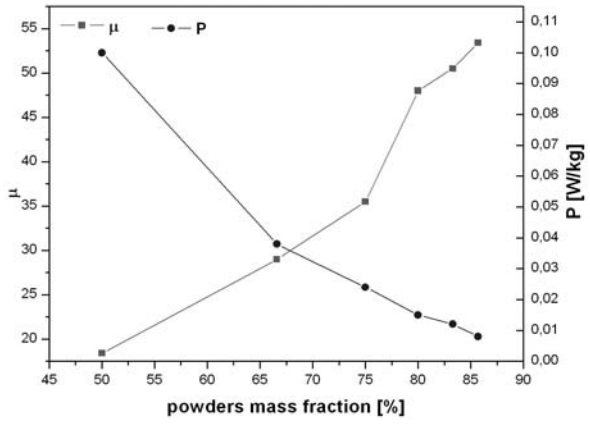

Fig. 24. Active power losses and magnetic permeability μ12000 of composites consisting Fe78Si9B13 powder as a function of powder mass share

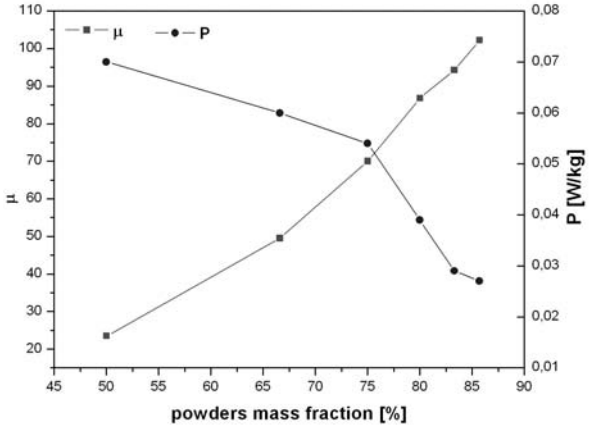

Fig.25. Active power losses and magnetic permeability μ12000 of composites consisting Fe73.5Cu1Nb3Si13.5B9 powder as a function of powder mass share

References

[1] M.E. McHenry, M.A. Willard, D.E. Laughlin, Amorphous and nanocrystalline materials for applications as soft magnets, Progress in Materials Science 44 (1999) 291-433.

[2] T. Bitoh, A. Makino, A. Inoue, The effect of grain-size distribution on coercivity in nanocrystalline soft magnetic alloys, Journal of Magnetism and Magnetic Materials 272-276 (2004) 1445-1446.

[3] Makino, T. Hatanai, A. Inoue, T. Masumoto, Nanocrystalline soft magnetic Fe-M-B (M=Zr, Hf, Nb) alloys and their applications, Materials Science and Engineering 226-228 (1997) 594-602.

[4] T. Kulik, J. Ferenc, M. Kowalczyk, Temperature of nanocrystallisation of magnetically soft alloys for high-temperature applications, Journal of Materials Processing Technology 162-163 (2005) 215-219.

[5] D. Szewieczek, J. Tyrlik-Held, S. Lesz, Changes of mechanical properties and fracture morphology of amorphous tapes involved by heat treatment, Journal of Materials Processing Technology 109 (2001) 190-195.

[6] P. Kwapuliński, J. Rasek, Z. Stokłosa, G. Haneczok, Magnetic properties of amorphous and nanocrystalline alloys based on iron, Journal of Materials Processing Technology 157-158 (2004) 735-742.

[7] Makino, A. Inoue, T. Masumoto, Soft magnetic properties of nanocrystalline Fe-M-B (M=Zr, Hf, Nb) alloys with high magnetization, Nanostructured Materials 6 (1995) 985-988.

[8] G. Bordin, G. Buttino, A. Cecchetti, M. Poppi, Temperature dependence of magnetic properties of a Co-based alloy in amorphous and nanostructured phase, Journal of Magnetism and Magnetic Materials 195 (1999) 583-585.

[9] S. Lesz, R. Nowosielski, B. Kostrubiec, Z. Stokłosa, Crystallization kinetics and magnetic properties of Co-based amorphous alloys, Journal of Achievements in Materials and Manufacturing Engineering 16 (2006) 35-39.

[10] D. Szewieczek, S. Lesz, The structure and selected physical properties of the nanocrystalline FeHfB alloy, Journal of Materials Processing Technology 157-158 (2004) 771-775.

[11] Suryanarayana, Mechanical alloying and milling, Progress in Materials Science 46 (2001) 1-184.

[12] R. Nowosielski, W. Pilarczyk, Structure and properties of Fe-6.67% C alloy obtained by mechanical alloying, Journal of Materials Processing Technology 162-163 (2005) 373-378.

[13] Bahrami, H.R. Madaah Hosseini, P. Abachi, S. Miraghaei Structural and soft magnetic properties of nanocrystalline $Fe_{85}Si_{10}Ni_5$ powders prepared by mechanical alloying, Materials Letters 60 (2006) 1068-1070.

[14] R. Nowosielski, L.A. Dobrzański, P. Gramatyka, S. Griner, J. Konieczny, Magnetic properties of high-energy milled $Fe_{78}Si_{13}B_9$ nanocrystalline powders and powder-based nanocomposites, Journal of Materials Processing Technology 157-158 (2004) 755-760.

[15] P. Gramatyka, R. Nowosielski, The synthesis of nanopowders by ball milling of metallic glasses, Proceedings of International Conference „Advances in Nanostructured Materials, Processing - Microstructure - Properties" NANOVED 2006 - NENAMAT, Stara Lesna, Slovakia, 2006, 81.

[16] Lebourgeois, S. Berenguer, C. Ramiarinjaona, T. Waeckerle, Analysis of the initial complex permeability versus frequency of soft nanocrystalline ribbons and derived composites, Journal of Magnetism and Magnetic Materials 254-255 (2003) 191-194.

[17] F. Mazaleyrat, L.K. Varga, Ferromagnetic nanocomposites, Journal of Magnetism and Magnetic Materials 215-216 (2000) 253-259.

[18] M. Muller, A. Novy, M. Brunner, R. Hilzinger, Powder composite cores of nanocrystalline soft magnetic FeSiB-CuNb alloys, Journal of Magnetism and Magnetic Materials 196-197 (1999) 357-358.

[19] Chicinas, O. Geoffroy, O. Isnard, V. Pop, Soft magnetic composite based on mechanically alloyed nanocrystalline Ni_3Fe phase, Journal of Magnetism and Magnetic Materials 290-291 (2005) 1531-1534.

[20] Lebourgeois, S. Berenguer, C. Ramiarinjaona, T. Waeckerle, Analysis of the initial complex permeability versus frequency of soft nanocrystalline ribbons and derived composites, Journal of Magnetism and Magnetic Materials 254-255 (2003) 191-194.

[21] Ziębowicz, D. Szewieczek, L.A. Dobrzański, Magnetic properties and structure of nanocomposites of powder $Fe_{73.5}Cu_1Nb_3Si_{13.5}B_9$ alloy-polymer type, Journal of Materials Processing Technology 157-158 (2004) 776-780.

[22] Szewieczek, L.A. Dobrzański, B. Ziębowicz, Structure and magnetic properties of nanocomposites of nanocrystalline powder-polymer type, Journal of Materials Processing Technology 157-158 (2004) 765-770.

[23] L.A. Dobrzański, R. Nowosielski, J. Konieczny, The structure and magnetic properties of magnetically soft cobalt base nanocrystalline powders and nanocomposites with silicon binding, Journal of Materials Processing Technology 155-156 (2004) 1943-1949.

[24] R. Nowosielski, J.J. Wysłocki, I. Wnuk, P. Sakiewicz, P. Gramatyka, Ferromagnetic properties of polymer nanocomposites containing $Fe_{78}Si_{13}B_9$ powder particles, Journal of Materials Processing Technology 162-163 (2005) 242-247.

[25] R. Nowosielski, J.J. Wysłocki, I. Wnuk, P. Gramatyka, Nanocrystalline soft magnetic composite cores, Journal of Materials Processing Technology 175 (2006) 324-329.